Numerical investigation of the impact of reflectors on spectral performance of Raman fibre laser

Elena G. Turitsyna*, Sergei K. Turitsyn, and Vladimir K. Mezentsev

Photonics Research Group, Aston University, Aston Triangle, Birmingham, B4 7ET, UK
**e.g.turitsyna@aston.ac.uk*

Abstract: Using a cavity mode model we study numerically the impact of bandwidth and spectral response profile of fibre Bragg gratings on four-wave-mixing-induced spectral broadening of radiation generated in 6 km and 22 km SMF-based Raman fibre lasers.

OCIS codes: (140.3550) Raman Lasers; (060.3735) Fiber Bragg gratings.

References and links

1. L. F. Mollenauer, and J. P. Gordon, *Solitons in Optical Fibers: Fundamentals and Applications* (Academic Press (2006).
2. A. Hasegawa, and Y. Kodama, *Solitons in Optical Communications* (Clarendon, Oxford, 1995).
3. V. E. Zakharov, and E. S. Wabnitz, *Optical Solitons: Theoretical Challenges and Industrial Perspectives* (Springer-Verlag, Heidelberg, 1998).
4. R. R. Alfano, *The Supercontinuum Laser Source: Fundamentals with Updated References* (Springer, New York, 2005)
5. M. Zheltikov, "Let there be white light: supercontinuum generation by ultra short laser pulses," Phys. Usp. **49**(6), 605 (2006).
6. J. Dudley, G. Genty, and S. Coen, "Supercontinuum generation in photonics crystal fibre," Rev. Mod. Phys. **78**(4), 1135–1184 (2006).
7. S. V. Smirnov, J. D. Ania Castanon, T. J. Ellingham, S. M. Kobtsev, S. Kukarin, and S. K. Turitsyn, "Optical spectral broadening and supercontinuum generation in telecom applications," Opt. Fiber Technol. **12**(2), 122–147 (2006).
8. J.-C. Bouteiller, "Spectral modeling of Raman fiber lasers," IEEE Photon. Technol. Lett. **15**(12), 1698–1700 (2003).
9. S. A. Babin, D. V. Churkin, A. E. Ismagulov, S. I. Kablukov, and E. V. Podivilov, "Four-wave-mixing-induced turbulent spectral broadening in a long Raman fiber laser," J. Opt. Soc. Am. B **24**(8), 1729–1738 (2007).
10. S. A. Babin, V. Karalekas, E. V. Podivilov, V. K. Mezentsev, P. Harper, J. D. Ania-Castañón, and S. K. Turitsyn, "Turbulent broadening of optical spectra in ultralong Raman fiber lasers," Phys. Rev. A **77**(3), 033803 (2008).
11. V. Karalekas, J. D. Ania-Castañón, P. Harper, S. A. Babin, E. V. Podivilov, and S. K. Turitsyn, "Impact of nonlinear spectral broadening in ultra-long Raman fibre lasers," Opt. Express **15**(25), 16690–16695 (2007), http://www.opticsinfobase.org/oe/abstract.cfm?URI=oe-15-25-16690.
12. E. G. Turitsyna, G. Falkovich, V. K. Mezentsev, and S. K. Turitsyn, "Optical turbulence and spectral condensate in long-fiber lasers," Phys. Rev. A **80**(3), 031804 (2009).
13. P. Suret, and S. Randoux, "Influence of spectral broadening on steady characteristics of Raman fiber lasers: From experiments to questions about validity of usual models," Opt. Commun. **237**(1–3), 201–212 (2004).
14. R. Vallée, E. Bélanger, B. Déry, M. Bernier, and D. Faucher, "Highly Efficient and High-Power Raman Fiber Laser Based on Broadband Chirped Fiber Bragg Gratings," J. Lightwave Technol. **24**(12), 5039–5043 (2006).
15. Y. Wang, and H. Po, "Characteristics of fibre Bragg gratings and influences on high-power Raman fibre lasers," Meas. Sci. Technol. **14**(6), 883–891 (2003).
16. V. E. Zakharov, V. S. L'vov, and G. E. Falkovich, *Kolmogorov Spectra of Turbulence I: Wave Turbulence* (Springer-Verlag, Berlin, 1992).
17. G. E. Falkovich, "Introduction to Turbulence Theory Lecture Notes on Turbulence and Coherent Structures in Fluids", Plasmas and Nonlinear Media Vol. 4 (World Scientific, Singapore, 2006).
18. J. D. Ania-Castañón, T. J. Ellingham, R. Ibbotson, X. Chen, L. Zhang, and S. K. Turitsyn, "Ultralong Raman fiber lasers as virtually lossless optical media," Phys. Rev. Lett. **96**(2), 023902 (2006).
19. J. D. Ania-Castañón, V. Karalekas, P. Harper, and S. K. Turitsyn, "Simultaneous Spatial and Spectral Transparency in Ultralong Fiber Lasers," Phys. Rev. Lett. **101**(12), 123903 (2008).

#119711 - $15.00 USD Received 9 Nov 2009; revised 7 Feb 2010; accepted 9 Feb 2010; published 19 Feb 2010

1. Introduction

In optical fibre, light waves are confined during propagation (that can take long distances) within the small core creating conditions for nonlinear medium response to travelling electric fields. Nonlinear fibre optics supplies the nonlinear science with a variety of examples of fundamental physical phenomena from solitons [1–3] to supercontinuum generation [4–7]. At the same time, effect of nonlinearity is a very practical issue with a direct impact on operation of fibre-based devices. In particular, effect of nonlinearity often manifests itself through a spectral broadening of radiation - a fundamental physical phenomenon that occurs in many practical optical systems (see e.g [4–7]. and references therein). Spectral broadening of generated radiation in fibre waveguide impacts performance of any fibre-based devices operating at high enough powers. Recent theoretical and experimental studies [8–12] of spectral broadening in some types of Raman fibre led to the conclusion that nonlinear four-wave-mixing (FWM) of the resonator modes is one of the key effects responsible for spectral broadening of laser radiation in the fibre cavity. The fibre laser cavity is typically formed by two fibre Bragg gratings (FBGs) acting as reflecting mirrors for the generated radiation at both edges of a fibre span. The FBG reflectors provide spectrally-selective cavity feedback. Effectively, the bandwidth of reflectors determines which longitudinal modes of a laser resonator are amplified and produce lasing. However, at high powers, due to nonlinear FWM interactions of the cavity modes, the radiation spectra broaden beyond the grating bandwidth leading to the power leakage out of the cavity and to degradation of the laser performance. It has been already understood that the effect of power overflow due to spectral broadening can be phenomenologically described as a decrease of the mean reflectivity of the FBG mirrors [13–15]. In [13] it was pointed out that the standard average power models used to describe Raman fibre lasers have to be modified to account for the effective power-dependent changes of the FBG reflectivity due to spectral broadening. In [15] using the average power models combined with a phenomenological approach accounting for power leakage it was studied how the FBG parameters (such as insertion loss, bandwidth and depth) affect the laser performance. Spectral broadening of radiation in fibre lasers is a nontrivial nonlinear effect having many similarities with wave turbulence [16, 17]. Therefore, modelling of fibre laser performance requires accurate accounting of interactions of a huge number of modes that is missing in the widely used average power models. In this work, through direct modelling of nonlinear interactions between laser modes, we examine the impact of the FBG bandwidth on spectral characteristics of the generated power and consider a possibility to control the laser performance through selection of optimal bandwidths. We study both cases of ultra-long Raman fibre lasers that can be used as quasi-lossless transmission medium [18, 19] and a Raman fibre laser with a shorter cavity of 6 km. We also consider here two types of FBG spectral response: Gaussian and Super-Gaussian shapes of the grating reflectivity.

2. Laser system scheme and basic model

The basic schematic design of an ultra-long Raman laser cavity described in details in [10–12, 18, 19] is schematically depicted in Fig. 1(a). The system consists of two equal-power pumps operating at 1365 nm and launched from both ends of a standard-single mode fibre (SMF) span. Two FBGs with high reflectivity (~99%), centered at 1455nm are positioned at either ends of the fibre span forming a high-Q cavity, trapping the radiation generated at 1455nm. Both Gaussian and Super-Gaussian (SG) FBGs are considered with varied bandwidths (measured as full width at half maximum) between 1 nm and 5 nm [Fig. 1(b)]. When the power of the primary pumps is above the required threshold for the stimulated Raman scattering gain to overcome the fibre attenuation, the cavity starts lasing at 1455 nm. Due to symmetry of the pumping scheme the generated radiation is evenly distributed in the cavity [18, 19]. This greatly simplifies theoretical analysis allowing us to approximate with good accuracy the gain distribution along the cavity as constant. In numerical modelling we use the cavity mode model described in details in [9]. The nonlinear FWM interactions of the multitude of the fibre laser resonator modes result in irregular temporal behaviour of the

#119711 - $15.00 USD Received 9 Nov 2009; revised 7 Feb 2010; accepted 9 Feb 2010; published 19 Feb 2010

generated radiation. Turbulent-like spectral broadening in Raman fibre lasers has been recently studied in [9–12]. Our goal here is to analyse in a consistent way how characteristics of the FBG reflectors (bandwidth and spectral shape) affect the generation and broadening of the laser radiation.

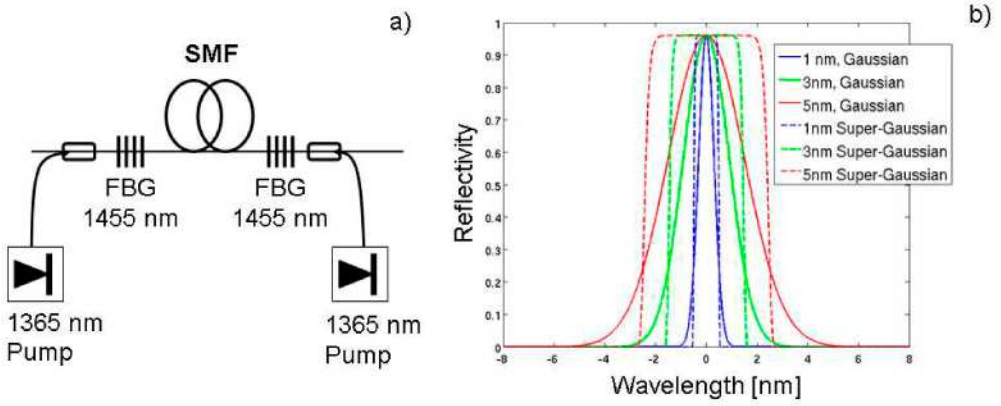

Fig. 1.(a) Schematic experimental setup; (b) Reflectivity profiles of considered FBGs: solid - Gaussian, dashed - Super-Gaussian.

Numerical modelling was performed using the master equation for the Fabry-Perot cavity mode envelopes E_m that has already shown good agreement with experimental results in different fibre laser systems [9, 10, 17–19]:

$$\frac{\tau_{rt}}{L}\frac{dE_m}{dt} = [g(P) - \alpha - \frac{\delta_m}{L} + i\beta_2\Omega_m^2]E_m - i\gamma\sum_{k,l} E_k E_l E_{k+l-m}^*$$

The terms in the right hand side describe the key physical effects in the fibre laser cavity: g(P) is the distributed Raman gain provided for radiation at 1455 nm by two symmetric pumps at 1365 nm and saturated at high total power $P = \sum_k |E_k|^2$ (see [9, 10, 19] for details); $\alpha = \alpha_{1455} = 0.25/8.66[km^{-1}]$ is the fibre loss at 1455 nm; $\delta_m = \delta_0 + \delta_2 \times m^2\Delta^2$ describes the combined effect of all lumped losses and the wavelength dependent FBGs losses, $\beta_2\,[ps^2km^{-1}]$ is the group velocity dispersion coefficient at 1455 nm, $\Omega_m = m\Delta[ps^{-1}]$ where $\Delta = \Omega/M$ is the spectral separation between modes in numerical modelling, Ω is the total spectral interval, M is the total number of modes used in numerical modelling to approximate the true cavity spectral mode separation with $\Delta[ps^{-1}] = 1.2955\,\Delta[nm]$, where $\Delta[nm] = \frac{\lambda^2}{c}\times\Delta\nu = \frac{\lambda^2}{2Ln}$; the nonlinearity parameter $\gamma = \frac{2\pi n_2}{\lambda A_{eff}} = 1.45[W^{-1}km^{-1}]$ describes effects of Kerr nonlinearity on the mode evolution. As it was found in [8–10], spectra of the generated radiation in the considered type of fibre lasers are determined by the four-wave nonlinear interactions of the cavity modes. The numerical window of $\Lambda = \lambda^2\Omega/(2\pi c) = 8[nm]$ (with some numerical runs using Λ as large as 18 nm depending on the FBG bandwidth) significantly exceeds the characteristic spectral width of the laser radiation in all cases used. In our numerical modelling we have employed $M = 2^{13}$ modes and have verified that neither changing this number up to $M = 2^{16}$, nor decreasing the time steps, nor increasing the window affect the results. Interactions of such a very large number of interacting modes sharing between them a finite generated power, demonstrate typical features of a wave turbulent behavior with characteristic power fluctuations and fast

#119711 - $15.00 USD Received 9 Nov 2009; revised 7 Feb 2010; accepted 9 Feb 2010; published 19 Feb 2010

randomisation of the phases of the resonator modes. In this work we examine the impact of the FBG bandwidth and spectral shape on spectral characteristics of the fluctuating generated power.

3. Results and discussion

When the total power from the primary pumps exceeds the required threshold for Raman-induced gain to overcome fibre attenuation at the Stokes wavelength, the cavity starts lasing at 1455 nm. Due to symmetry of the pumping scheme and the laser resonator, the generated radiation is evenly distributed along the cavity [18, 19]. Note that here we consider closed laser resonators without any out-coupling of power from the cavity. The results of numerical modeling are presented in Figs. 2–7.

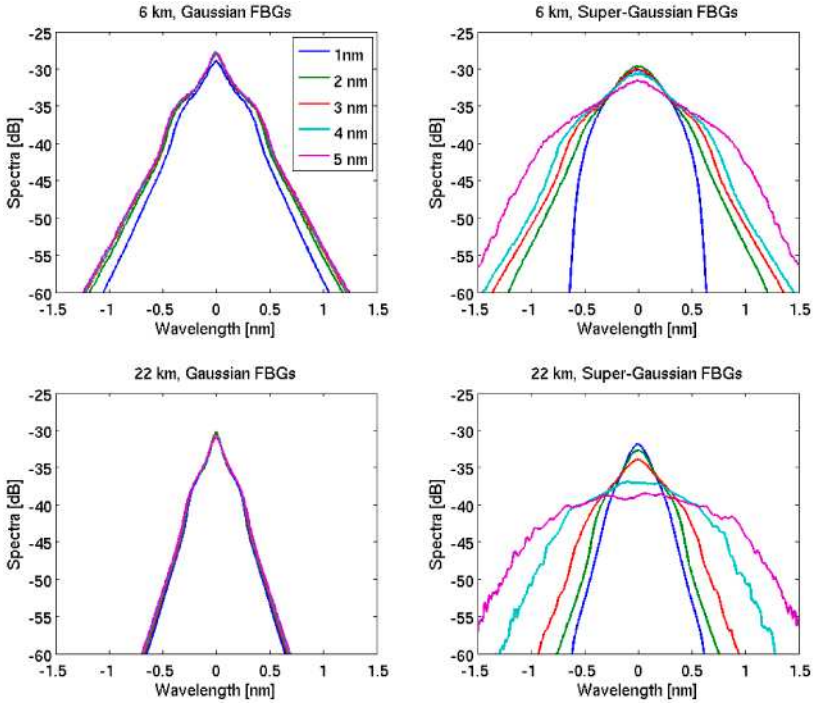

Fig. 2. Spectral power (in logarithmic scale) is shown for FBGs bandwidths varying from 1 to 5 nm and 600 mW total pump power. Upper pictures – 6 km laser, bottom – 22 km cavity.

In general, the generated radiation spectra are mostly determined by the nonlinear physical effects inside the cavity. However, it is also seen from Fig. 2 that the bandwidth and spectral response (shape) of the reflectors have impact on the spectral distribution of the generated power.

#119711 - $15.00 USD Received 9 Nov 2009; revised 7 Feb 2010; accepted 9 Feb 2010; published 19 Feb 2010

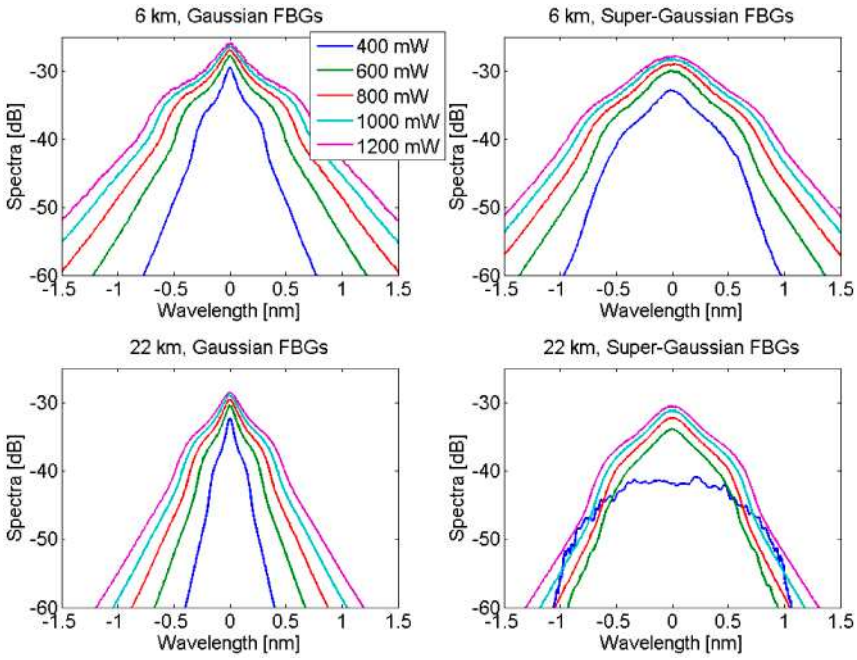

Fig. 3. Spectral power for 3nm FBGs and different pump powers.

First observation from Figs. 2 and 6 is that at the same total pump power (600 mW), for a shorter cavity laser (6 km here) the spectra are typically broader than for a longer cavity laser (here 22 km) for both Gaussian and Super-Gaussian spectral profiles of the reflectors. It is interesting to note that in the considered system, the bandwidth of the FBGs has very little impact on the generated spectra profile for Gaussian type gratings (Fig. 2 – left). However, in the case of the Super-Gaussian FBGs, change of the bandwidth affects the tails of the forming spectra (Fig. 2 – right). Note that even for 5 nm Super-Gaussian FBGs the generated spectra are still narrow compared to the reflector bandwidth. This means that the reflector's characteristics such as spectral response profile and bandwidth affect the nonlinear mode interactions well before the start of the process of a power overflow and leakage of radiation from the cavity due to spectral broadening beyond the FBG bandwidth. One of the key points that we would like to stress here is that building and stablisation of spectra of generated radiation in the considered long fibre lasers operating at high enough power regimes is determined by *kinetic,* rather than *dynamical* mechanisms. Power of the generated radiation is distributed between a huge number of longitudinal resonator modes leading to weak interactions between modes through four-wave mixing. As the result of such interaction, the phases of the interaction modes become random and irregular; behavior of such optical system resembles turbulent-like processes [16, 17, 9, 10, 12]. The longer the fibre laser cavity length is the more resonator modes are involved in such weak randomised interactions, and as the result - the pronounced effect of optical wave turbulence in the system.

#119711 - $15.00 USD Received 9 Nov 2009; revised 7 Feb 2010; accepted 9 Feb 2010; published 19 Feb 2010

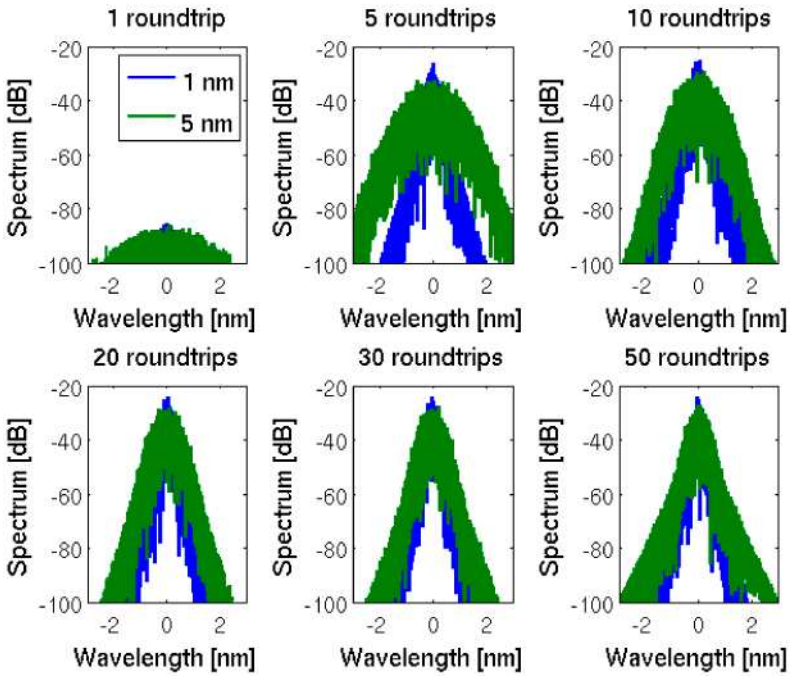

Fig. 4. Spectra generation for Gaussian FBGs with 1 and 5 nm bandwidth.

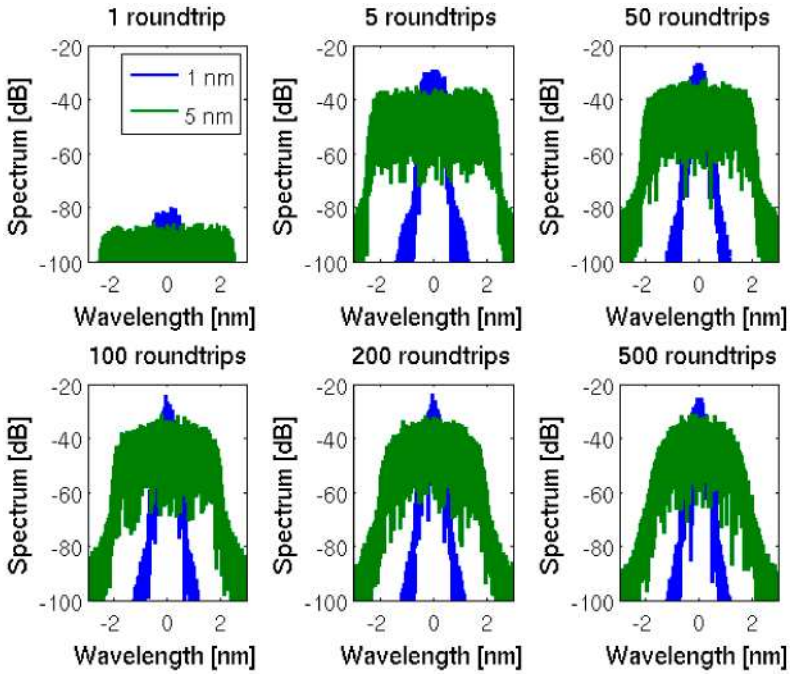

Fig. 5. Spectra generation for Super-Gaussian FBGs with 1 and 5 nm bandwidth.

Figures 3 and 6 show how the bandwidth and the total power of the generated radiation depend on the total pumping power. It is seen that Gaussian grating typically provides more narrow spectra compared to the case of a Super-Gaussian FBG. The impact of the reflector shapes on the building of optical wave turbulence that determines optical spectra (namely a

#119711 - $15.00 USD Received 9 Nov 2009; revised 7 Feb 2010; accepted 9 Feb 2010; published 19 Feb 2010

difference between Gaussian and Super-Gaussian FBGs) can be qualitatively understood in the following way. The key impact is more likely to originate from the behavior of the resulting gain curve near the maximum, which is sharper in the case of the Gaussian FBG, and is more flat in the case of Super-Gaussian FBG. The optical turbulence spectra result from the cascaded interactions starting from the group of the most amplified modes that are narrower in the case of the Gaussian-shaped reflectors.

Analysis of the process of generation and building of the radiated spectra (Fig. 4, 5) shows that at the same pump power (600 mW) for Gaussian FBGs with 1 and 5 nm bandwidth the spectra stabilise in about 20-30 roundtrips and remain almost identical after that; whereas for Super-Gaussian FBGs it takes much longer for the spectra to stabilise. It is also seen from Figs. 4 and 5 that in the case of Gaussian FBG profile, the reflectors' bandwidth does not affect strongly the asymptotic spectrum, but in the case of the Super-Gaussian reflector, the generated spectrum follows more closely the bandwidth of the gratings (Fig. 5, after 500 round trips).

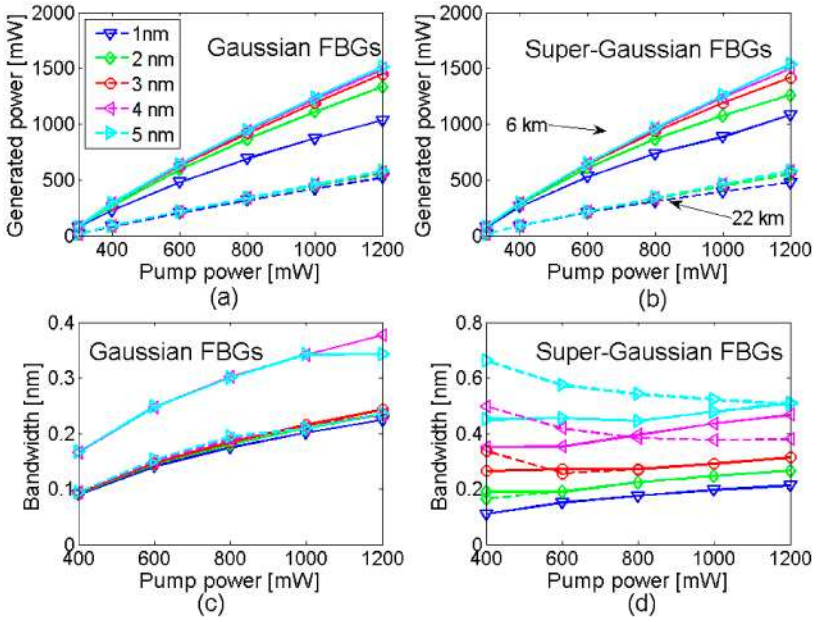

Fig. 6. Total generated power (a, b) and root mean square bandwidth (c, d) versus the total pump power for different FBGs. Solid lines - 6 km laser, dashed lines - 22 km cavity.

Figures 6 and 7 demonstrate that in the case of more narrow gratings, the ratio between generated power and pump power is lower compared to the case of broader gratings, in agreement with the observations in [15]. We would like to stress once more that the observed behavior should be understood in terms of turbulent-like kinetic mechanisms related to optical wave de-phasing and randomisation, rather than in terms of dynamical interpretation of wave interactions. Note, that in the case of 6 km laser and pump powers larger than 800 mW, the effective nonlinearity/dispersion ratio $\xi = \gamma P / (|\beta_2| \Omega_{RMS}^2)$, where Ω_{RMS} is the root-mean-square spectral width of the asymptotic radiation state, is larger than unity for both Gaussian and Super-Gaussian FBGs. This means that the laser operates in the regime of developed optical wave turbulence as discussed in [12]. Comprehensive theoretical analysis and interpretation of the underlying physical mechanisms of the observed results are still to be developed.

#119711 - $15.00 USD Received 9 Nov 2009; revised 7 Feb 2010; accepted 9 Feb 2010; published 19 Feb 2010

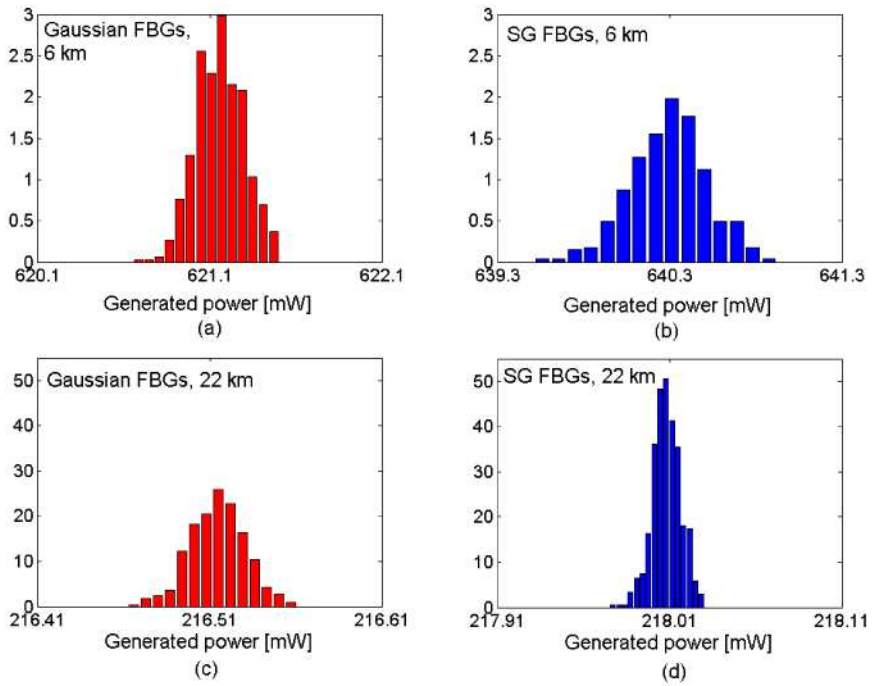

Fig. 7. Normalised histograms of generated power for Gaussian (a,c) and Super-Gaussian (b,d) FBGs and 6 km (a,b) and 22-km (c,d) cavity lengths. Here the total pump power is 600 mW and FBGs with 3 nm bandwidth is used.

Figure 7 shows the impact of the laser cavity length and reflectors' shape on the fluctuations of the total generated power in time. Interestingly, for 3 nm grating bandwidth, in the case of the Gaussian-shaped reflectors, the level of fluctuations is larger for longer cavity, while in the case of the Super-Gaussian gratings the situation is opposite. A longer fibre cavity leads to more resonator modes involved in weak FWM interactions, and lower effective distributed average power making turbulent properties of spectra different to a shorter laser.

4. Conclusion

We have studied how properties of FBG-based reflectors, such as bandwidth and spectral shape influence the spectral features of the radiation generated in 6-km and 22-km Raman fibre lasers. We have demonstrated that, though general properties of the generated spectra are mostly determined by the nonlinear physical effects inside the cavity, shape and bandwidth of the FBG reflectors have impact on spectral properties of the generated radiation. On the one hand, a spectral width of the FBGs response has a direct impact through interactions with spectra of the Stokes wave that at high generated power might experience spectral broadening and overflow beyond the gratings bandwidth [13]. On the other hand, the reflector's bandwidth impacts through the filtering effect, the balance between the cavity nonlinearity and dispersion that is sensitive to the spectral width of the wave packet generated in the resonator. We have observed that for a shorter laser with 6 km cavity the broadening level is higher than in 22 km fibre laser resonator. This can be explained by the larger total loss in a longer cavity and, as the result, a smaller effective average nonlinearity. In the case of a Super-Gaussian grating profile, the spectral width of the generated radiation is strongly affected by the FBG bandwidth, while for a Gaussian FBG there is no strong dependence on the gratings' bandwidth. We have found that when using a narrow (1 nm) SG FBG the spectrum of the generated radiation can be kept very narrow even for high input powers. We have observed that in the case of Gaussian FBGs and 22 km laser

#119711 - $15.00 USD Received 9 Nov 2009; revised 7 Feb 2010; accepted 9 Feb 2010; published 19 Feb 2010

cavity the generated power level is less sensitive to the grating bandwidth. An increase of the Gaussian FBG bandwidth beyond 2 nm does not lead to the increase in the ratio of the total generated power to the total pump power. However, in the case of the Super-Gaussian FBG the level of generated power follows the grating bandwidth. This gives some new design opportunities for better control of the spectral properties of generated laser radiation and shows that optimization of the FBGs bandwidth in shorter lasers is important for control of spectral performance.

Acknowledgments

The authors acknowledge the Royal Society support through the Dorothy Hodgkin Fellowship and the Royal Society Wolfson Merit Fellowship.

#119711 - $15.00 USD Received 9 Nov 2009; revised 7 Feb 2010; accepted 9 Feb 2010; published 19 Feb 2010